American Journal of Human Biology

WILEY

American Journal of Human Biology

ORIGINAL ARTICLE OPEN ACCESS

Revealing Developmental Transitions in Perinatal and Infant Individuals Through Microanatomical Analysis

María Molina Moreno[1,2] | Danielle M. Doe[2] | Nieves Candelas González[2] | Daniel García Martínez[3] | Armando González Martín[2,4] | Oscar Cambra-Moo[2,4]

[1]Grup de Recerca en Antropología Biològica (GREAB), Departament de Biología Animal, Biología Vegetal i D'ecología, Universitat Autònoma de Barcelona, Barcelona, Spain | [2]Laboratorio de Poblaciones del Pasado (LAPP), Departamento de Biología, Universidad Autónoma de Madrid, Madrid, Spain | [3]Complutense University of Madrid Faculty of Biological Sciences, Department of Biodiversity, Ecology, and Evolution, Madrid, Spain | [4]Grupo de Investigación en Arqueología Antigua y Medieval (ARQUEOS), Universidad de Oviedo, Oviedo, Spain

Correspondence: María Molina Moreno (maria.molina.moreno@uab.cat)

Received: 15 January 2025 | **Revised:** 9 June 2025 | **Accepted:** 19 June 2025

Funding: This work was supported by JDC2022-049244-I, (Ministerio de Ciencia, Innovación y Universidades and Next Generation UE) UAM CA4/RSUE/2022-00292 (Ministerio de Universidades, Plan de Recuperación, Transformación y Resiliencia) and FPI-UAM 2017 predoctoral funding. The Laboratorio de Poblaciones del Pasado (LAPP) has been supported by Projects PGC2018-099405-B-100, HAR2017-82755-P, HAR2017-83004-P, HAR2016-78036-P, HAR2016-74846-P (Spanish Government), a grant (ref. 38360) from The Leakey Foundation and SI4/PJI/2024-00104 (Comunidad de Madrid) and by the Ministerio de Ciencia, Innovación y Universidades.

Keywords: birth | bone histology | full-term | microanatomy | prenatal

ABSTRACT

Objectives: Identifying signs of birth in perinatal human remains of past populations is challenging due to the lack of direct markers of this event on bones. This research aims to identify distinct events in humeral cross-sections microanatomy related to perinatal development and to integrate the findings into infant mortality trends.

Material and Methods: The sample consists of infants ($N = 106$) ranging from prenatal to 1.5 years, with microanatomical analysis of nine selected individuals. Age-at-death estimation and microanatomical characterization were conducted, combined with quantitative analysis of microanatomical features.

Results: Biological age-at-death presents high variability and overlap across prenatal to postnatal stages. Microanatomical analysis reveals a higher percentage of mineralized areas (60%–80%) within the total cross-sectional area in the youngest individuals up to the first neonatal month.

Conclusions: Based on the integration of microanatomical analysis in an extensive infant sample, this study highlights the evidence of developmental transitions from prenatal to neonatal stages. These findings suggest that, unlike biological age estimation methods, the full-term period can be identified microanatomically in bone. This provides a valuable approach for analyzing fragmented skeletal remains, secondary deposits, and other funerary or osteological contexts, opening new pathways to understand gestational development and postnatal survival in past populations.

1 | Introduction

A major challenge in bioarcheological studies is accurately defining the timing of birth in perinatal individuals from past populations, which has important social and biological implications. The type of fetal death and burial, and determining if the baby was full-term, preterm, or small for gestational age (SGA), are key indicators of maternal health and the overall well-being

Armando González Martín and Oscar Cambra Moo should be considered joint senior author.

of populations (Lewis 2006; Blake 2018; Halcrow et al. 2018). Although typical gestation lasts between 37 and 42 weeks (258–293 days), referred to as full-term (Scheuer et al. 2000), most births occur around 38 weeks (Jukic et al. 2013). The challenge lies in determining the moment of birth in fetal and perinatal individuals in the absence of a specific chronological age (González Martín 1998), which serves as a crucial reference point for accurately categorizing individuals. This study employs widely accepted age category definitions based on various recognized references (Monnier 1985; Scheuer et al. 2000; Lewis 2006) to make this study comparable, reproducible, and appropriate when referring to biological age and developmental status (Figure 1).

While the fetal period technically ends at birth, identifying fetuses from neonates, or even stillborn or live-born individuals, is challenging as this event leaves no direct markers on bones (Blake 2018). Within archaeological populations, in utero individuals constitute the sole direct evidence of fetuses (unborn) in the past (Halcrow 2020). Unlike postnatal individuals, whose remains are more commonly recovered and studied, fetal individuals are rarely identified unless they are found within the burial context of pregnant women (Rascón Pérez et al. 2007; Malgosa et al. 2016; De Miguel Ibáñez 2018; De Miguel Ibáñez et al. 2021; Armentano et al. 2020; Halcrow 2020; Molina Moreno 2021; Doe et al. 2022; among others). Concerning the isolated buried babies, one of the most reliable ways to infer birth is through dental histology by observing the neonatal line, which forms when enamel development pauses during delivery (Zanolli et al. 2011; Kurek et al. 2016; Martirosyan et al. 2024). However, this line may vary depending on factors like delivery type (e.g., cesarean) or gestational age at birth (Eli et al. 1989). Through age-at-death estimation, it may also be possible to determine if an individual likely died before or after birth. Whenever possible, age estimation based on the dentition is recommended over skeletal age as teeth are generally less affected by environmental conditions (Moorrees et al. 1963). In the absence of dental analysis, age-at-death estimation relies on skeletal size, growth, and development (Fazekas and Kósa 1978; Scheuer et al. 1980, 2000).

In terms of skeletal development, bone histology has significantly contributed to our knowledge of past human populations by analyzing the organization and composition of bone at the microscopic level (Enlow 1963; Stout and Crowder 2012). Osteon counts and the size and density of Haversian canals, a technique known as histomorphometry, are used to estimate the age of adult individuals (Stout and Crowder 2012). Some studies have also employed this methodology for age estimation in non-adult individuals (Baltadjiev 1995; Streeter 2010; Valencia et al. 2020). In fetal individuals specifically, early tibial development shows a high density of osteons, fewer thick lamellae, wide Haversian canals, and thin bone layers, while later gestation is characterized by decreased osteon density, narrower and fewer Haversian canals, and thicker intercanal bone layers (Baltadjiev 1995).

In this context, histomorphological characterization and the quantification of microanatomical features have been effectively employed in anthropological research to investigate diverse questions in both the fossil and archaeological records, such as ontogenetic changes, skeletal emaciation, and taphonomy (Goldman et al. 2005, 2009; Cambra-Moo et al. 2012, 2014; Schug and Goldman 2014; García-Martínez et al. 2017; García-Gil et al. 2018; García Gil 2021). Ontogenetic changes were first described in the tibia and humerus based on the percentages of mineralized versus non-mineralized tissue (Cambra-Moo et al. 2012, 2014). Similar differences in the percentages of microstructure have been observed in the human skull and humerus, with higher percentages of mineralized area in the parietal bone (García-Gil et al. 2018; García Gil 2021). Analogous findings have been obtained in the axial skeleton, where histological and micro-CT analyses of the thoracic cage have shown differences in compartmentalization throughout ontogeny (García-Martínez et al. 2017; López-Rey et al. 2022, 2024). Finally, in the femur, malnutrition has been identified based on cross-section shape and microanatomical features related to bone size at different ages during infancy (Schug and Goldman 2014). A common finding across all this research is the differentiation in the percentages of mineralized tissue area in individuals classified as perinatal.

Building on these findings related to skeletal mineralization across developmental stages, it is essential to consider the unique processes of mineral transport and accumulation during the prenatal period. Fetal mineral transport and

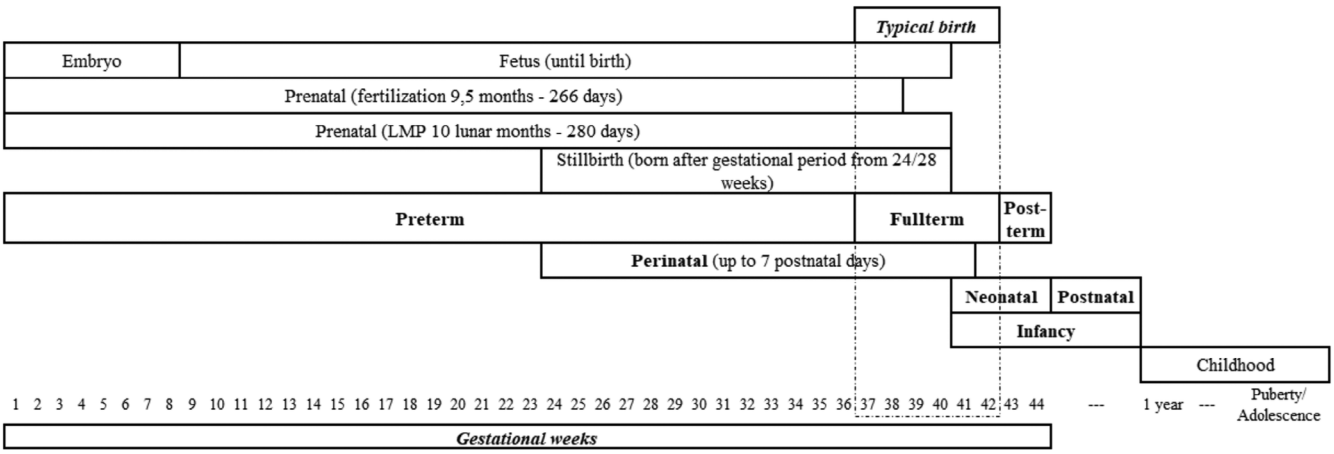

FIGURE 1 | Age categories based on Monnier (1985), Scheuer et al. (2000) and Lewis (2006). The reference of 40 gestational weeks has been considered in categories that consider the moment of birth (fetus, perinatal, neonatal, stillbirth, postnatal and infancy).

metabolism are uniquely adapted to ensure that the skeleton is fully mineralized before birth. To meet the high demands of the rapidly mineralizing fetal skeleton, calcium, magnesium, and phosphorus are actively transported across the placenta (Givens and Macy 1933; Shaw et al. 1990). Unlike adults, during fetal development, the intestines, kidneys, and bones do not serve as the primary sources of minerals. Instead, the placenta is responsible for supplying the necessary minerals to effectively achieve skeletal mineralization before birth (Ryan and Kovacs 2020). Although the accumulation process begins in the first months of gestation, it peaks during the third trimester, with 80% of the total body calcium volume accrued in this period (Givens and Macy 1933; Trotter and Hixon 1974; Ryan et al. 1988; Ryan and Kovacs 2020). After birth, neonates must quickly adapt their regulation of mineral homeostasis because they lose the placental calcium supply. The newborn continues to accumulate skeletal calcium at a similar rate to a late-term fetus. Consequently, they rely on intestinal calcium intake, skeletal calcium stores, and renal calcium reabsorption to maintain normal blood calcium levels while experiencing ongoing rapid skeletal growth. During childhood, skeletal mass grows due to both linear growth and alterations in bone dimensions and density (DiMeglio and Leonard 2013).

This study investigates prenatal and early infant mortality in past populations through the analysis of skeletal remains from 106 perinatal and infant individuals recovered from various Spanish archaeological sites. We focus on how bone microanatomy (specifically, the microstructural organization of the humerus) can complement traditional dental-based age-at-death estimation to improve our understanding of biological maturity at the time of death. We aim to (1) establish refined age-at-death estimations using well-documented dental development timelines; (2) assess histological features of bone tissue in a subsample of nine perinatal individuals to identify markers potentially linked to developmental stage or birth status; and (3) evaluate the potential of bone histology as a tool for interpreting the perinatal mortality of these populations by integrating these data with age-at-death estimations. By applying this combined approach to archaeological material, we aim to contribute to the understanding of birth and death in our individuals and offer complementary alternatives to study and interpret early life mortality in non-individualized or poorly contextualized burial settings.

2 | Material and Methods

2.1 | Sample

The infant sample consists of 106 individuals in the prenatal, perinatal, and early infancy stages, from which a microanatomical sample of 9 individuals was derived. The non-adult skeletons in the larger infant sample have been fully analyzed anthropologically in previous studies (González Martín 1999; Candelas González et al. 2016; Molina Moreno 2021; Candelas González 2023). Excavated from ten Spanish archaeological sites spanning the Bronze Age (III millennium BC) to the 19th century, the burials cover different funerary practices according to their chrono-cultural context. Further information of the whole sample is provided in Table S1. Age ranges covered include prenatal individuals to 1.5 years, based on dental and skeletal age-at-death estimation (Ubelaker 1978; Fazekas and Kósa 1978; Scheuer et al. 1980) (Figure 2).

The microanatomical sample ($n = 9$) was carefully selected to analyze prenatal and perinatal microstructure development, specifically compared with early infancy. For this reason, three of the individuals were recovered from maternal-fetal burials (Baza, San Nicolás, and Lugo de Llanera) (Rascón Pérez et al. 2007; Doe et al. 2022) and six from La Encantada archaeological site (Galán Saulnier and Sánchez Meseguer 2019; Molina Moreno 2021). Additional information about these individuals is provided in Table S2. Since the first three represent confirmed cases of prenatal death (they were determined to have died around or before 280 gestational days and were found in the context of pregnant women's burials), the other six perinatal and infant individuals were intended to offer a comparative reference covering all stages, from prenatal to postnatal periods. The results of these nine individuals were then considered within the context of the broader perinatal and early infancy mortality group.

2.2 | Biological Age-At-Death Estimation

Age-at-death estimation for the entire infant sample ($N = 106$) was performed using the quantitative method of Irurita Olivares and colleagues, which is based on the dimensions of dental germs from the documented osteological collection of Granada, Spain (Irurita Olivares et al. 2014). This method was found to be the most accurate for deciduous dentition in Iberian Peninsula archaeological samples and is preferred over other quantitative age-at-death estimation methods (Molina Moreno 2021). In two cases—maternal/fetal burials Baza 52.1 and LL(A)77.1—where the dentition was absent, linear equations for the humerus maximum length were used (Scheuer et al. 1980). The results aligned with previous biological age estimates for these individuals (Rascón Pérez et al. 2007; Molina Moreno 2021; Doe et al. 2022).

The length of dental germs was measured perpendicular to the occlusal surface, as described by Liversidge et al. (1993). A digital caliper with an experimental error of 0.1 mm was used. A total of 665 dental germs were measured, each of which has been subjected to the corresponding regression equation (Irurita Olivares et al. 2014), obtaining maximum,

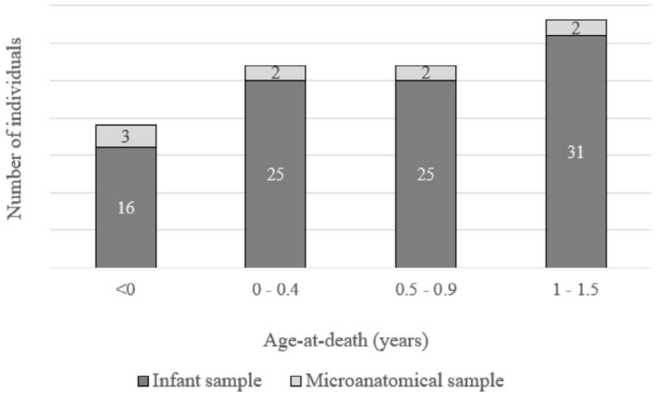

FIGURE 2 | Age distribution of the infant sample ($N = 97$) and the microanatomical sample ($N = 9$).

minimum, mean, and error range values for the estimation of age at death. Measurement accuracy was verified through an interobserver error analysis conducted on the second inferior molar, using 20 pairwise measurements of randomly selected individuals. Repeatability of dental measurements was analyzed statistically using the Intraclass Correlation Coefficient (ICC) test (SPSS IBM Statistics v. 26.0. Armonk, NY: IBM Corp.). The age estimation was based on multiple teeth (anterior and molar teeth, upper and lower), and the final age was calculated as the average of the estimated ages from all available teeth. The error range was set as the minimum and maximum values of the estimated ages to cover the full range of possibilities regarding the estimated age, minimizing any errors that might exist in the estimation.

To enable comparison across the entire sample, individuals with gestational ages (up to 280 days) were represented using negative values. Specifically, 280 days were subtracted from the gestational age estimated using the method by Irurita Olivares et al. (2014), allowing these individuals to be accurately positioned to the left of zero on the timeline. For instance, an individual estimated at 220 gestational days (corresponding to the 32nd gestational week) is plotted as-60 days, indicating the number of days remaining until full-term (280 days).

2.3 | Microanatomical Study

Microanatomy was analyzed in the midshaft humeri of the subsample ($N = 9$). As histological methods are inherently destructive, the humeri were carefully measured, photographed, and 3D scanned so they could be available for future research. Maximum length of the humerus was taken following the appropriate methods for non-adult individuals (Fazekas and Kósa 1978; Buikstra and Ubelaker 1994) and scans were taken using an Artec Spider 3D device in the Virtual Morphology Laboratory of the National Museum of Natural Sciences (MNCN, CSIC). The 3D models were exported in'.ply' format, printed, and are currently stored in the *Laboratorio de Poblaciones del Pasado* (Biology Department, UAM). The midpoint of the diaphysis was calculated based on the maximum length of the humerus in complete bones. When incomplete, it was estimated using the length of the contralateral side. In cases where both humeri were incomplete, the cut point was marked immediately below the nutrient foramen as it is the closest area to the midpoint. Once the cut point was determined, 0.5 cm was marked on each side to perform a transverse cut of the diaphysis.

Thin sections were prepared in collaboration with the *Instituto de Cerámica y Vidrio* (ICV-CSIC), following the protocol previously used in other archaeological human bones (Cambra-Moo et al. 2012, 2014; García-Martínez et al. 2017; García-Gil et al. 2018; García Gil 2021), using a two-component resin (EpoFix resin and EpoFix Hardener, Struers, Cleveland, Ohio, USA). Notably, we made a transverse cut at the midshaft of 1 cm (instead of 1.5 cm) and thin sections were polished using cloths of different grits (from 120 to 4000) until the thickness of the section was reduced to approximately 100 μm, following the standards described in Bromage et al. (2003). The sections were observed and photographed under a polarized light microscope (Olympus CX31 microscope equipped with an OMAX digital camera A35100U camera). Between 30 and 205 photographs were taken per individual of the entire area of the humerus section. A complete photomontage of each section was created using Photoshop CS6 (Adobe Systems, San Jose, USA).

Bone tissues were classified based on known vascularization patterns and bone matrix organization (Francillon-Vieillot et al. 1990; McFarlin et al. 2016). Spatial terms such as cortex—referring to the external, peripheral part of a long bone—and medullary region—referring to the internal or central part—were used to ease the description of microstructural features (Enlow 1963; Francillon-Vieillot et al. 1990). The original bone tissue preserved is expressed in terms of percentage (Millard 2001; Hollund et al. 2012).

Quantitative histological analysis of the total area of the humerus was performed to describe the histomorphological characteristics in numerical terms per unit area analogous to osteometry. Following previously described protocols (Cambra-Moo et al. 2012, 2014; García-Martínez et al. 2017; García-Gil et al. 2018), we drew and quantified a total of 3656 polygons corresponding to vascular channels, medullary cavity, and total area of each thin section with the Geographic Information System (GIS) software (ArcMap 10.8.2, Esri, Redlands, California, USA). Then, we calculated the percentage of the total area, the area occupied by mineralized tissue (Min.Ar), and the total area not occupied by mineralized tissue (nMin.Ar), calculated from the sum of the medullary canal area and vascular cavities areas. These values were expressed as the Compartmentalization Index (Comp. Index), the ratio of mineralized to non-mineralized tissue area (López-Rey et al. 2022, 2024). The higher the result of the Comp. Index, the greater the proportion of area occupied by mineralized tissue (Min.Ar) compared to the area occupied by the medullary canal and vascular cavities (nMin.Ar). An interobserver error was estimated (from Molina Moreno 2021:213) based on the standard deviation of the values measured by a second observer on an unknown thin section, including the map, areas, and relative percentages (Figure S1).

The Comp. Index was used to compare our results to other studies which have explored mineralized areas in cross-sections of long bones such as the humerus (Cambra-Moo et al. 2014) and femur (Schug and Goldman 2014). To standardize the age-at-death of the individuals for comparison, data were recalculated, assigning a biological age-at-death based on humeri following Maresh (1970) and Scheuer et al. (1980). Further information on the recalculated age is provided in Table S3.

3 | Results

3.1 | Biological Age-At-Death

The characterization of the entire infant sample, based on the quantitative estimation of biological age, reveals the progression of a measured variable across different age categories, starting from the prenatal stage up to 24 months of age (Figure 3). The high level of agreement in the interobserver error test (ICC = 0.999, F value = 4358.184, $p < 0.05$) supports the consistency of the observations.

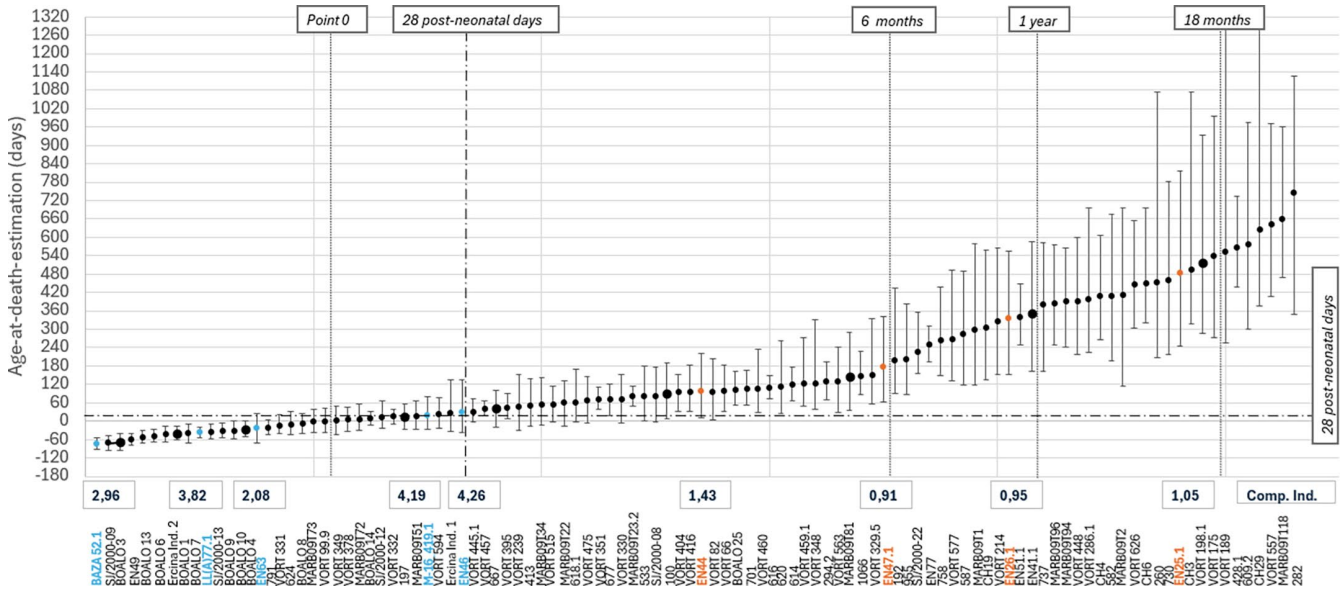

FIGURE 3 | Biological age-at-death range distribution of the sample of 106 archaeological individuals belonging to a wider study group (Molina Moreno 2021). Individuals histologically analyzed are highlighted in blue (with higher Comp. Index values) and red (with lower Comp. Index values). Age is expressed in days. Every individual has its own range according to the results obtained (Scheuer et al. 1980; Irurita Olivares et al. 2014).

Two key findings arise from this analysis (Figure 3). First, as age increases, the error bars show greater variability. Second, there is a significant overlap between age groups, illustrating the lack of clear distinction among prenatal, perinatal, neonatal, and postnatal categories. The trend line demonstrates that age-at-death estimation starts negative or near zero in the prenatal group (36 days before birth) and steadily increases in subsequent age groups. The 0–28 days group has a mean of 17 postnatal days, which exceeds early neonatal age. For older individuals, confidence intervals widen, highlighting increased variability with age. The "14–24 months" group peaks with measured values between 800 and 1000 postnatal days, suggesting a significant rise over time.

Analyzing the average age of the sample shows that 21 individuals died during the prenatal period, while 12 died in their first month of life and were consequently classified as neonatal (Figure 3). Individual 419.1, identified from a maternal-fetal burial and categorized as unborn, falls within this neonatal group (average age of 19 postnatal days). This indicates that the categories of prenatal, perinatal, neonatal, and postnatal are indistinguishable using the biological age estimation methods used.

3.2 | Microanatomical Analysis

Among the potential categories for classifying bone tissue types, specific types were identified based on the organization of collagen fibers and the arrangement of vascularization. Birefringence allowed for the observation of the organization and arrangement of collagen fibers. However, matrix areas showing widespread destruction or infiltrations in the form of stains could not be examined due to these alterations. This limitation affected individuals LL(A)77.1, M-16_419.1, EN47.1, EN26.1, and some areas of EN25.1 (Figure 4b,d,g,h,i).

Baza 52.1, LL(A)77.1, and EN63 (Figure 4a–c) exhibited tissue purely categorized as woven bone, indicative of the initial formation of the matrix. Osteocytic lacunae were clearly visible in Baza 52.1 and EN63 due to their high percentage of preserved intact bone (Figure 4a,c). Subsequently, individuals with generalized woven bone matrix (M-16_419.1, EN46) began showing areas with greater complexity in the arrangement of collagen fibers and the organization of vascular channels, tending toward parallel-fibered bone in the anterior surface of the bone, specifically in the anteromedial (Figure 4d,e). However, from two post-neonatal months onward, individual EN44 presented the greatest complexity of the bone matrix, which shifted to the posterior region (Figure 4f). Individuals EN26.1 and EN47.1 (Figure 4g,h) could not be fully evaluated because of the greatest alteration of the microstructure. In any case, we identified the presence of secondary osteons (SO) in the posterior area of EN47.1, meaning that remodeling processes have already started. Finally, the oldest individual, EN25.1 (Figure 4i), seemed to present an incipient lamellar tissue in the medial and posteromedial regions.

With respect to the microanatomical quantitative analysis, it was possible to quantify the morphological characteristics independent of intact tissue percentages. The standard deviation of each quantified area was between 0.01 (section area) and 0.1 (vascularization), indicating a low error (Further information is provided in Figure S1). The highest proportions of mineralized tissue area (from 67% to 81%) corresponded to the youngest individuals, with average age-at-death estimations from 29 weeks in utero to the first month. These individuals, including M-16_419.1 and EN46, showed a greater presence of early formation tissue (woven bone) in their microstructure (Figure 4a–e) and the highest Comp. Index values (> 4) (Table 1). From this point, the ratio of mineralized tissue area decreased to almost 1:1 (50%). This change in proportions was reflected in the increase of the space occupied by the medullary cavity. As the size

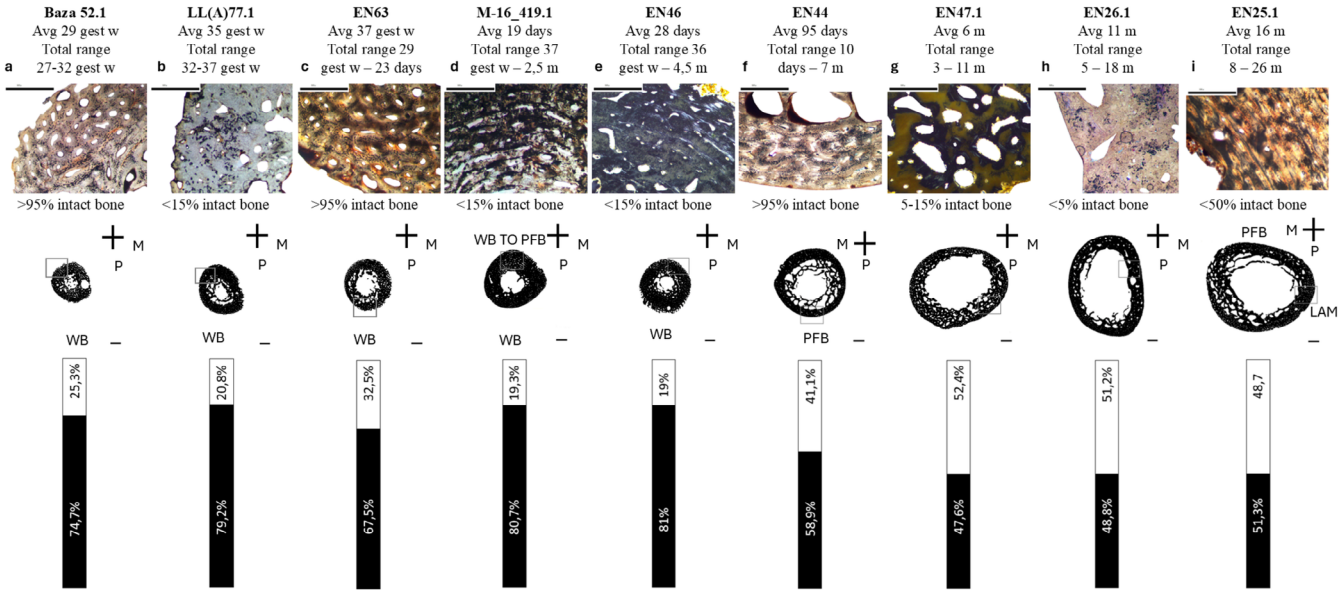

FIGURE 4 | Histological maps, percentages of Min.Ar and nMin.Ar and tissue detail of the humeri cross-sections. Biological age-at-death estimation range and average in this study has already been included in the figure. (a) Baza 52.1, polarized light, ¼ μ wave plate, (b) LL(A)77.1 normal light, (c) EN63 polarized light. (d) M-16_419.1, polarized light, (e) EN46 polarized light, (f) EN44 polarized light. (g) EN47.1, polarized light, (h) EN26.1 normal light, (i) EN25.1 polarized light. WB = Woven Bone. M = Medial, *P*=Posterior. Detailed images scale bar = 500 μ, map's scale bar = 1 mm.

TABLE 1 | Histomorphological data from humeri expressed in mm^2 and percentages.

					nMin.Ar					
					Medullary canal		Vascularization		Total nMin.Ar	
N° individual	Comp. Index	Section area mm^2	Min.Ar mm^2	%	mm^2	%	mm^2	%	mm^2	%
BAZA 52.1	2.96	10.31	7.70	74.73	0.97	9.44	1.63	15.82	2.60	25.27
LL(A)77.1	3.82	16.73	13.26	79.24	1.56	9.32	1.91	11.43	3.47	20.76
EN63	2.08	16.05	10.83	67.48	3.45	21.51	1.77	11.01	5.22	32.52
M-16_419.1	4.19	22.79	18.40	80.74	3.31	14.54	1.08	4.72	4.39	19.26
EN46	4.26	21.08	17.08	81.00	2.15	10.19	1.86	8.81	4.01	19.00
EN44	1.43	32.83	19.34	58.90	7.07	21.53	6.41	19.52	13.48	41.05
EN47.1	0.91	52.62	25.02	47.56	23.36	44.40	4.23	8.04	27.59	52.44
EN26.1	0.95	59.58	29.05	48.76	27.45	46.07	3.08	5.17	30.53	51.24
EN25.1	1.05	68.33	35.04	51.28	26.38	38.61	6.91	10.11	33.29	48.72

Note: Vascularization refers to all empty areas except the medullary canal.

and thickness of the humerus increase, growth of the medullary cavity is expected, but when comparing the proportions, it was possible to observe that this structure occupied a greater percentage of the total section area, while the vascular cavities remained uniform throughout the sample. Only individual EN44, diagnosed with rickets (González Martín et al. 1999), presented a degree of vascularization equivalent to that of the medullary cavity.

Microstructure analysis, combined with the entire infant sample mortality trends (Figure 3), revealed that individuals with the highest mineralized area percentages were found before or within the first neonatal month (Baza 52.1, LL(A)77.1, EN63, M-16_419.1, and EN46). Individuals M-16_419.1 and EN46 had mean ages at death of 19 and 28 days, respectively, coinciding with the highest Comp. Index values (> 4) (Table 1). A reduction in mineralized tissue area was evident later in individual EN44, around the fourth postnatal month (95 postnatal days), with the progression continuing in older individuals (EN47.1, EN26.1, EN25.1), reflecting increased vascularization of the humerus up to 16 months in individual EN25.1. (Figure 5). As the objective of this analysis was to show the tendency that aligns with the majority of the dataset, individual EN63 has been excluded because of its visual deviation.

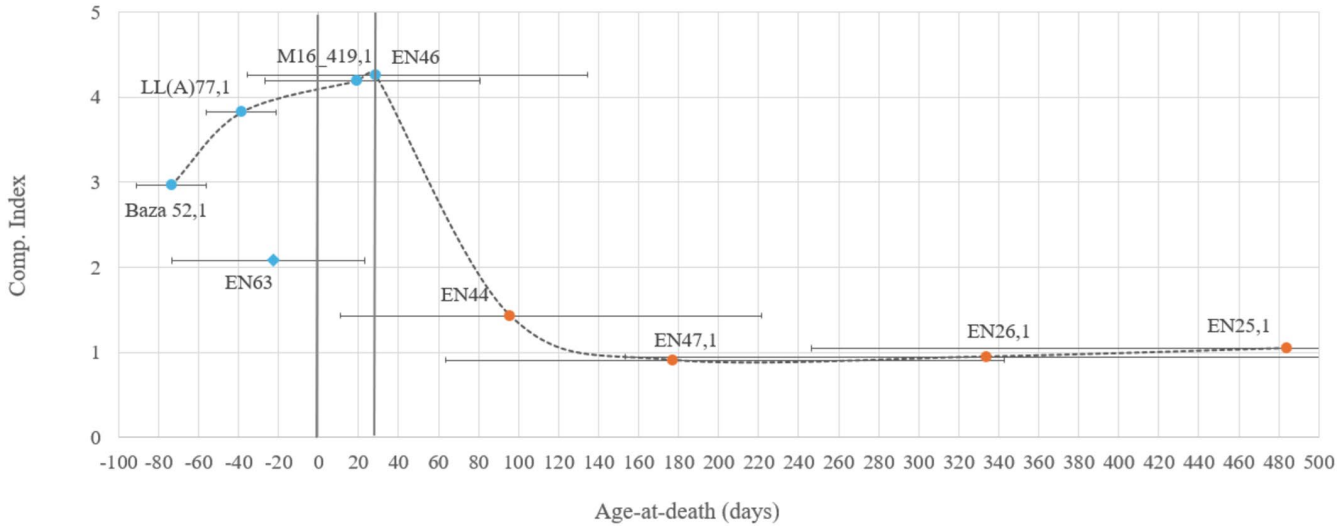

FIGURE 5 | Evolution of the Comp. Index with biological age-at-death estimation (days) of microanatomical sample ($N = 9$). Individual EN63 has been excluded of the tendency line analysis based on its visual deviation from the trend.

4 | Discussion

Since birth leaves no direct evidence on bones (Blake 2018), various histological approaches have been undertaken, ranging from dental histology (Eli et al. 1989; Zanolli et al. 2011; Martirosyan et al. 2024) to ontogenetic changes in different anatomical regions (Goldman et al. 2005, 2009; Cambra-Moo et al. 2012, 2014; García-Martínez et al. 2017; García-Gil et al. 2018; García Gil 2021). This study presents a novel histological approach that combines anthropological and microanatomical characterization to analyze the changes in the areas occupied by mineralized and non-mineralized tissues during the perinatal and early infancy stages specifically.

Although the lack of antemortem clinical data is inherent to bioarcheology, it is important to consider that perinatal and infant individuals are particularly susceptible to environmental changes and maternal health (Lewis 2006; Hodson and Gowland 2020; Halcrow 2020). Six of the individuals selected for microanatomical analyses were found in isolation. Based on the premise that they had already been born, whether alive or deceased, any direct interpretation of maternal health was impossible. However, the significance of the selected individuals in this study lies in the fact that three of them originate from burial contexts of pregnant women, representing the only confirmed fetuses in archaeological contexts (Rascón Pérez et al. 2007; Malgosa et al. 2016; De Miguel Ibáñez 2018; De Miguel Ibáñez et al. 2021; Armentano et al. 2020; Halcrow 2020; Molina Moreno 2021; Doe et al. 2022); an evaluation of the health status of the mothers was possible. In this context, linear enamel hypoplasia (LEH) was identified in all three mothers, which may indicate subpar nutrition or illness during infancy and childhood (Lewis 2006). Specifically, in the case of Baza 52, dental caries and calculus were also observed, indicating overall poor oral health. Additionally, bilateral cribra femoral was identified, pointing to periods of nutritional and health-related stress during later childhood and pregnancy (Rascón Pérez et al. 2007; Doe et al. 2022). Baza 52.1 is the most developmentally immature individual, with an estimated gestational age of 27–32 weeks, which could potentially be related to compromised maternal health.

The selection of the sample is intended to represent unborn individuals from the prenatal stage (Baza 52.1 and LL(A) 77.1), full-term stage (M-16_419.1) and individuals who died during the perinatal and infant stages (EN63, EN46, EN44, EN47.1, EN26.1 and EN25.1). Although the microanatomical sample size is limited due to the use of destructive techniques, the integration of anthropological and histomorphological data establishes a valuable contribution to understanding bone development in the moments before and after birth in these archaeological populations.

The infant sample ($N = 106$) originates from the Iberian Peninsula, offering a geographically coherent study population. However, the inclusion of individuals from different sites and periods introduces variability due to the influence of diverse socio-cultural and economic contexts, which may have shaped patterns of infant growth and biological development (Lewis 2006; Hodson and Gowland 2020; Halcrow 2020). This variability represents a limitation in making broad comparisons. Nevertheless, the study provides a valuable framework for understanding early life development, with important implications for forensic anthropology and non-individualized osteoarcheological contexts, such as secondary deposits, ossuaries, or mass graves.

4.1 | Peak of Mineralized Tissue Areas in the Full-Term Period

Microstructural analysis revealed that individuals with peak mineralized tissue percentages were found exclusively within or prior to the first neonatal month (individuals marked as blue in Figure 3). In spite of microstructure preservation limiting the observation of bone tissue types in many individuals, it is worth noting that it was possible to quantify the microanatomical features of all individuals. Thus, quantitative analysis offers

an advantage and provides precise information regardless of the preservation of the histological section. In this respect, drawing humeral cross-sections of perinatal and infant individuals has enabled the quantification of the areas of mineralized tissue relative to the areas occupied by non-mineralized tissue (medullary canal and vascular cavities), relating these measurements with bone tissue types and establishing an equivalence with the age-at-death estimation. In this regard, it has been possible to identify a high Comp. Index (4:1) in the youngest individuals, which coincides with a widespread presence of woven bone and an average age ranging from the intrauterine stage to the first neonatal month of development.

These results coincide with previous studies that have also detected a higher percentage of mineralized tissue area in perinatal individuals (Cambra-Moo et al. 2014; Schug and Goldman 2014; García-Martínez et al. 2017). A thorough comparison based on the calculation of the Comp. Index between the humerus and the femur has confirmed that this higher concentration of mineralized tissue area corresponds to the moment around birth, during the perinatal stage. Femoral cross-sections were consistently larger than those of the humeri in perinates and infants, yet the Comp. Index showed similar proportions among individuals of the same age-at-death groups, with the highest levels in the perinatal stage, especially in the femur (Comp. Index: 5.29) (data from Schug and Goldman 2014) (Figure S2).

Mechanical influences have been suggested to affect the bone volume fraction (bone volume/trabecular volume) in the humerus, tibia, and femur. These values start out very high in neonatal individuals, decline to a minimum around one year of age, and then progressively increase again to adult levels through development (Gosman 2012). This phenomenon is well known in medicine, has been attributed to the need to achieve full mineralization of the skeleton before birth (Givens and Macy 1933; Shaw et al. 1990), and is maintained in neonatal individuals (DiMeglio and Leonard 2013). Based on the results presented here, the authors suggest that this phenomenon can be observed through the study of microanatomy related to the highest percentages of mineralized tissue area in the humerus of the perinatal and neonatal individuals, associated with periods of stillbirth and neonatal mortality in clinics (Monnier 1985).

Although biological age cannot be directly equated to chronological age (Lewis 2006), we have also observed a minor difference between those biologically determined as "pre-term" and "full-term" in their microanatomical quantifications. Three individuals categorized as pre-term (Baza 52.1, LL(A)77.1 and EN63) presented a Comp. Index = 2 – 3.83 (70% mineralized tissue area). All of them have a mean age corresponding to the third trimester of intrauterine development, coinciding with the described mineralization accumulation in the medical literature (Givens and Macy 1933; Trotter and Hixon 1974; Ryan and Kovacs 2020). Furthermore, those individuals at term, with a mean age situated in the first neonatal month (M-16_419.1 and EN46), are those exhibiting the highest Comp. Index (> 4, > 80% of mineralized tissue area). Considering that individual M-16_419.1 was unborn (Molina Moreno 2021; Doe et al. 2022) and, therefore, probably post-term, this study likely reflects the peak of mineralization of a full-term individual that reaches these values in the humerus, consistent with similar postnatal calcium accumulation rates (DiMeglio and Leonard 2013) and observed in the humeri and femur of other populations (Cambra-Moo et al. 2014; Schug and Goldman 2014). Further information of the data compared is available in Table S4 and Figure S2.

From the third postnatal month onward, the Comp. Index decreases significantly by half, represented not only by individual EN44, but also in the other comparative populations (Cambra-Moo et al. 2014; Schug and Goldman 2014). However, the pathological condition of individual EN44 (González Martín et al. 1999) necessitates caution in interpretation. Even so, from 6 to 24 months, the ratio remains around 1:1, indicating an increase in the medullary canal in particular. This is understandable because throughout childhood, skeletal mass increases due to both lineal growth and changes in bone dimensions and density. Although there is an initial decrease in mineral bone density in the months after birth, it is succeeded by an increase that continues into adulthood (DiMeglio and Leonard 2013). Indeed, percentages around 53% and 67% have been observed in the adult humerus (Cambra-Moo et al. 2014).

4.2 | Contributions of Microanatomy to the Study of Age-at-Death in Perinatal Individuals

The integration of microanatomical analysis for a representative subsample within a larger sample of over one hundred individuals provides critical insights into perinatal and early infant mortality in Iberian archaeological populations. While the infant sample ($N = 106$) includes biological age estimations, the detailed microanatomical subsample ($N = 9$) offers refined data on developmental stages, particularly around birth and the first neonatal month or post-term stage (until 44 gestational weeks, Figure 1). These individuals, showing peaks in mineralized tissue percentages, enhance the accuracy of age-at-death estimations, helping to understand the transition from prenatal to postnatal life. This level of precision is crucial, especially for individuals like M-16_419.1 and EN46, in which age ranges are tightly constrained to the weeks before and after birth. In this sense, microanatomy reveals observable changes, such as the reduction of area occupied by mineralized tissue and increased vascularization after the neonatal period, that are otherwise invisible in standard biological age assessments. Since the limited microanatomical sample size presents a challenge for generalization, this study aims to provide preliminary insights into a more accurate and comprehensive understanding of perinatal mortality across the entire sample.

The neonatal transition from the intrauterine gestational environment to the extrauterine is difficult, as organs must function independently from the mother (Bogin 2021). The newborn's intestines, kidneys, and the skeleton become responsible for feeding and provisioning of minerals, including calcium (Ryan and Kovacs 2020). The exploration of microanatomy allows us to determine that this process is not only visible in teeth (Kurek et al. 2016) but also in archaeological bones, highlighting differences between individuals in gestational development and full-term or newborn stages.

Comparisons with other studies confirm these results, not only in the humerus but also in the lower limbs and the ribcage

(Cambra-Moo et al. 2014; Schug and Goldman 2014; García-Martínez et al. 2017; García-Gil et al. 2018). Higher percentages in the femur could be related to greater mechanical stress from weight-bearing and locomotion, resulting in increased cortical thickness (Gosman 2012). The skull, mandible, and ribs have an intramembranous embryonic formation, while limb bones have an endochondral origin (Scheuer et al. 2000). In spite of this, the ribs show similar results to the limb bones, but not the vault bones (García-Gil et al. 2018; García Gil 2021). Besides the necessity for complete mineralization of the skeleton before birth, hormonal processes could also influence these developmental patterns, this event observable in the microstructure mineralized area percentages, similar to that seen during adolescence (García-Gil et al. 2018).

Although new methods of estimating chronological age are being explored that present a narrower estimated range, such as odontochronology (Zanolli et al. 2011; Kurek et al. 2016; Martirosyan et al. 2024), the authors emphasize the importance of this study not only in terms of the development of microstructure in past populations, but also as an ontogenetic approach to gestational development, natural mortality timing, and early infancy. The ability to establish a pattern derived from the Comp. Index and the percentage of mineralized tissue areas from any limb bone allows for valuable information on development in cases of fragmented skeletal remains or incomplete and taphonomically altered individuals. Additionally, being able to identify whether an individual has reached full-term or is in an earlier or later stage, confirmed by the remains of maternal/fetal burials (Molina Moreno 2021; Doe et al. 2022), opens a new avenue of understanding regarding survival after birth. Specifically, it provides insight into survival beyond the first neonatal month, having surpassed the clinical period of natural mortality (Monnier 1985).

Naturally, future research should explore this line of inquiry using larger samples and non-destructive imaging techniques such as micro-CT scan (López-Rey et al. 2022; García-Martínez et al. 2023), which have shown promising results in terms of the study of the Comp. Index in perinatal and infant individuals (García-Martínez et al. 2023). However, histological analysis provides critical information that cannot be visualized through micro-CT alone, such as the detailed development of bone tissues or the presence of osteocyte lacunae (Francillon-Vieillot et al. 1990; Millard 2001; Hollund et al. 2012; McFarlin et al. 2016). Microstructure transitions toward more mature tissue types, such as parallel-fibered bone in full-term individuals, offer valuable insights that cannot be obtained from scanning techniques to date. Finally, the exploration of other anatomical units will help verify most of the mineralized tissue in late-term individuals throughout the perinatal skeleton. This broader examination will provide a more comprehensive understanding of skeletal development during this critical stage, contributing to more accurate interpretations in a bioarchaeological context.

5 | Conclusions

Despite preservation challenges, histomorphological quantitative analysis allowed for accurate quantification of microanatomical features across individuals. A high Comp. Index has been identified in younger individuals, ranging from the intrauterine period to the first neonatal month, aligned with previous studies identifying a higher percentage of mineralized tissue area in perinatal individuals. Specifically, we suggest that the microstructure shows a peak of mineralized tissue areas in the full-term individuals of this study, coinciding with the period of maximum mineral transfer to the fetus to ensure a fully mineralized skeleton before birth. Therefore, microanatomy appears to show evidence of the transition from the intrauterine to extrauterine developmental environment, closely related to the stillbirth and neonatal period associated with natural mortality.

This study underscores the value of microanatomical analysis in understanding gestational development, mortality timing, and early infancy in archaeological populations, aiding in age-at-death estimation in fragmented or taphonomically altered skeletal remains and providing insights into survival beyond the neonatal period. Future research should employ non-destructive imaging techniques and compare findings with individuals of known age and sex to further validate and expand these insights across different anatomical units.

Author Contributions

María Molina Moreno: conceptualization (equal), data curation (supporting), formal analysis (lead), funding acquisition (equal), investigation (lead), methodology (equal), software (equal), validation (equal), visualization (equal), writing – original draft (lead), writing – review and editing (equal). **Danielle M. Doe:** data curation (equal), formal analysis (supporting), methodology (supporting), writing – review and editing (equal). **Nieves Candelas González:** data curation (equal), formal analysis (supporting), methodology (supporting), writing – review and editing (equal). **Daniel García Martínez:** data curation (supporting), visualization (equal), writing – review and editing (equal). **Armando González Martín:** conceptualization (lead), data curation (lead), funding acquisition (lead), investigation (lead), methodology (equal), project administration (lead), resources (lead), supervision (lead), writing – review and editing (equal). **Oscar Cambra-Moo:** conceptualization (lead), data curation (lead), funding acquisition (lead), investigation (lead), methodology (equal), project administration (lead), resources (equal), software (lead), supervision (lead), writing – review and editing (equal).

Acknowledgments

This Project has been funded by JDC2022-049244-I, (Ministerio de Ciencia, Innovación y Universidades and Next Generation UE) UAM CA4/RSUE/2022-00292 (Ministerio de Universidades, Plan de Recuperación, Transformación y Resiliencia) and FPI-UAM 2017 predoctoral funding. The *Laboratorio de Poblaciones del Pasado* (LAPP) has been supported by Projects PGC2018-099405-B-100, HAR2017-82755-P, HAR2017-83004-P, HAR2016-78036-P, HAR2016-74846-P (Spanish Government), a grant (ref. 38360) from The Leakey Foundation and SI4/PJI/2024-00104 (Comunidad de Madrid).

We extend our gratitude to Miguel Ángel Rodríguez Barbero (ICV-CSIC) for providing the facilities for the preparation of the thin sections, Orosia García Gil (UAM) for the initial training in thin section sample preparation and the humeri interobserver error, the MNCN (CSIC) for creating the 3D models of the humeri, Lucía Villaescusa (UAM) for the teeth interobserver error, and Josefina Rascón Pérez (UAM) for the archaeological intervention in Veranes and maternofetal individuals. We also thank Catalina Galán Saulnier, José Sánchez Meseguer, Carmen Fernández Ochoa (UAM), José Avelino Gutiérrez (UNIOVI), Fernando Gil Sendino, Javier Salido Domínguez (UAM), Rosario Gómez Osuna, Fernando Muñoz Villarejo, Emilio Campomanes Alvaredo, and Paloma García Díaz for granting

permission to the LAPP for the investigation of the osteoarchaeological collections included in this study.

Ethics Statement

The human remains examined in this study are part of various established osteological collections that were excavated under proper institutional supervision and lack identifiable descendant groups, making community consultation impossible given their historical and anonymous nature. Ethical clearance for this research has been previously granted by the Comité de Ética de la Investigación (CEI) of the Universidad Autónoma de Madrid, which has formally approved the use of this collection for research purposes.

Conflicts of Interest

The authors declare no conflicts of interest.

Data Availability Statement

The data that support the findings of this study are available from the corresponding author upon reasonable request.

References

Armentano, N., D. Nociarová, M. Esqué, et al. 2020. "L'accouchement tragique de Lucy? À propos de la mortalité maternofoetale de la préhistoire à l'époque médiévale." *Gynécologie Obstétrique Fertilité & Sénologie* 48, no. 2: 204–210.

Baltadjiev, G. 1995. "Micromorphometric Characteristics of Osteons in Compact Bone of Growing Tibiae of Human Fetuses." *Cells, Tissues, Organs* 154, no. 3: 181–185.

Blake, K. A. 2018. "The Biology of the Fetal Period: Interpreting Life From Fetal Skeletal Remains." In *The Anthropology of the Fetus*, edited by S. Han, T. K. Betsinger, and A. B. Scott, 34–58. Berghahn Books.

Bogin, B. 2021. *Patterns of Human Growth*. Third ed. Cambridge University Press.

Bromage, T. G., H. M. Goldman, S. C. McFarlin, J. Warshaw, A. Boyde, and C. M. Riggs. 2003. "Circularly Polarized Light Standards for Investigations of Collagen Fiber Orientation in Bone." *Anatomical Record* 274, no. B: 157–168.

Buikstra, J. E., and D. H. Ubelaker. 1994. "Standards for Data Collection from Human Skeletal Remains. Arkansas Archaeological Survey Research Series N° 44, Arkansas."

Cambra-Moo, O., C. Nacarino Meneses, M. Á. Rodríguez Barbero, et al. 2012. "Mapping Human Long Bone Compartmentalisation During Ontogeny: A New Methodological Approach." *Journal of Structural Biology* 178, no. 3: 338–349.

Cambra-Moo, O., C. Nacarino Meneses, M. Á. Rodríguez Barbero, et al. 2014. "An Approach to the Histomorphological and Histochemical Variations of the Humerus Cortical Bone Through Human Ontogeny." *Journal of Anatomy* 224, no. 6: 634–646.

Candelas González, N., A. Núñez Cantalapiedra, J. Rascón Pérez, et al. 2016. "Características paleodemográficas de la población recuperada del cementerio de Marialba de la Ribera (Villaturiel, León, España) (S. IV–XIII)." *Munibe Antropologia-Arkeologia* 67: 151–165.

Candelas González, N. 2023. "Historia biológica de las poblaciones humanas del territorio astur entre época antigua y medieval. Los individuos no-adultos del yacimiento de Marialba de la Ribera (Unpublished doctoral dissertation). Universidad Autónoma de Madrid, Madrid."

De Miguel Ibáñez, M. P. 2018. "En la frontera de lo invisible. Las muertes maternas a partir de la documentación arqueológica en Navarra." *Trabajos de Arqueología Navarra* 30: 215–235.

De Miguel Ibáñez, M. P., T. Majó, M. Díaz – Zorita Bonilla, M. Ramos Aguirre, J. Sesma, and J. Siles. 2021. "Un cas de mortalité maternelle dans le cimitière du monastère de Fitero (XIVe – XVIe siècles) (Navarre, Espagne)." In *Rencontre autour du corps malade. Prise en charge et traitement funéraire des individus souffrants à travers les siècles. Actes de la 10e Rencontre du Gaaf, 23–25 mai 2018: Gaaf 10*, edited by S. Kachi, H. Réveillas, and C. J. Knüsel, 306–310. Gaaf 10.

DiMeglio, L. A., and M. B. Leonard. 2013. "Bone Mineral Acquisition *in Utero* and During Infancy and Childhood." In *Osteoporosis*, edited by R. Marcus, D. Feldman, D. W. Dempster, M. Luckey, and J. A. Cauley, 4th ed., 977–1015. Elsevier Academic Press.

Doe, D. M., M. Molina Moreno, N. Candelas González, J. Rascón Pérez, O. Cambra-Moo, and A. González Martín. 2022. "First Application of a Puberty Estimation Method to Skeletons of Young Pregnant Females: A Case for the Reevaluation of Maternal–Fetal Burials." *International Journal of Osteoarchaeology* 32, no. 2: 418–428.

Eli, I., H. Sarnat, and E. Talmi. 1989. "Effect of the Birth Process on the Neonatal Line in Primary Tooth Enamel." *Pediatric Dentistry* 11, no. 3: 220–223.

Enlow, D. H. 1963. *Principles of Bone Remodeling: An Account of Post-Natal Growth and Remodeling Processes in Long Bones and the Mandible*. Charles C. Thomas Publisher Ltd.

Fazekas, I. G., and F. Kósa. 1978. *Forensic Fetal Osteology*. Akadémiae Kiadó.

Francillon-Vieillot, H., V. de Buffrénil, J. Castanet, et al. 1990. "Microstructure and Mineralization of Vertebrate Skeletal Tissues." In *Skeletal Biomineralization: Patterns, Processes and Evolutionary Trends*, edited by J. G. Carter, 471–530. Van Nostrand Reinhold.

Galán Saulnier, C., and J. L. Sánchez Meseguer. 2019. *Tumbas infantiles en el Cerro de La Encantada*. Arkatros Ediciones.

García Gil, O. 2021. "Modelado y remodelado en los huesos del neurocráneo (Unpublished doctoral dissertation). Universidad Autónoma de Madrid, Madrid."

García-Gil, O., J. Audije-Gil, O. Cambra-Moo, et al. 2018. "Evaluation of Macro- and Micro-Taphonomic Preservation of Non-Adult Remains From the Hispano-Muslim Maqbara of San Nicolás (Murcia, Spain) Reveals Overall Poor Skeletal Micropreservation and New Histomorphological Data." In *ISPH 2017 Fourth International Symposium on Paleohistology. PostSymposium Publication*, edited by R. A. Pellegrini and D. C. Parris, 50–60. New Jersey State Museum Investigations.

García-Martínez, D., O. García Gil, O. Cambra-Moo, et al. 2017. "External and Internal Ontogenetic Changes in the First Rib." *American Journal of Physical Anthropology* 164, no. 4: 750–762.

García-Martínez, D., J. M. López-Rey, O. G. Gil, et al. 2023. "How Accurate Are Medical CT and Micro-CT Techniques Compared to Classical Histology When Addressing the Growth of the Internal Rib Parameters?" *Anthropologischer Anzeiger* 80, no. 3: 307–316.

Givens, M. H., and I. G. Macy. 1933. "The Chemical Composition of the Human Fetus." *Journal of Biological Chemistry* 102, no. 1: 7–17.

Goldman, H. M., S. C. McFarlin, D. M. Cooper, C. D. L. Thomas, and J. G. Clement. 2009. "Ontogenetic Patterning of Cortical Bone Microstructure and Geometry at the Human Mid-Shaft Femur." *Anatomical Record* 292, no. 1: 48–64.

Goldman, H. M., C. D. L. Thomas, J. G. Clement, and T. G. Bromage. 2005. "Relationships Among Microstructural Properties of Bone at the Human Midshaft Femur." *Journal of Anatomy* 206, no. 2: 127–139.

González Martín, A. 1998. "El Babel terminológico: ¿Neonatos, precoces, fetos, mortinatos, a término o muertos al nacimiento?" *Boletín de la Asociación Española de Paleopatología* 19: 4–6.

González Martín, A. 1999. "Infancia y adolescencia en la Murcia musulmana: estudio de restos óseos (Unpublished doctoral dissertation). Universidad Autónoma de Madrid, Madrid."

González Martín, A., M. Campo Martín, F. J. Robles Rodríguez, and I. Pastor Abascal. 1999. "Evidencias paleopatológicas de raquitismo en España." In *Sistematización metodológica en Paleopatología. Actas del V Congreso Nacional de la Asociación Española de Paleopatología*, edited by J. A. Sánchez Sánchez, 139–145. Asociación Española de Paleopatología.

Gosman, J. H. 2012. "Growth and Development. Morphology, Mechanisms and Abnormalities." In *Bone Histology: An Anthropological Perspective*, edited by C. Crowder and S. Stout, 23–44. CRC Press.

Halcrow, S. E. 2020. "Infants in the Bioarchaeological Past: Who Cares?" In *The Mother-Infant Nexus in Anthropology. Bioarchaeology and Social Theory*, edited by R. Gowland and S. E. Halcrow, 19–38. Springer.

Halcrow, S. E., N. Tayles, and G. E. Elliot. 2018. "The Bioarchaeology of Fetuses." In *The Anthropology of the Fetus*, edited by S. Han, T. K. Betsinger, and A. B. Scott, 83–111. Berghahn Books.

Hodson, C. M., and R. Gowland. 2020. "Like Mother, Like Child: Investigating Perinatal and Maternal Health Stress in Post-Medieval London." In *The Mother-Infant Nexus in Anthropology. Bioarchaeology and Social Theory*, edited by R. Gowland and S. E. Halcrow, 39–64. Springer.

Hollund, H. I., M. M. E. Jans, M. J. Collins, H. Kars, I. Joosten, and S. M. Kars. 2012. "What Happened Here? Bone Histology as a Tool in Decoding the Postmortem Histories of Archaeological Bone From Castricum, The Netherlands." *International Journal of Osteoarchaeology* 22, no. 5: 537–548.

Irurita Olivares, J., I. Alemán Aguilera, J. Viciano Badal, S. De Luca, and M. C. Botella López. 2014. "Evaluation of the Maximum Length of Deciduous Teeth for Estimation of the Age of Infants and Young Children: Proposal of New Regression Formulas." *International Journal of Legal Medicine* 128, no. 2: 345–352.

Jukic, A. M., D. D. Baird, C. R. Weinberg, D. R. McConnaughey, and A. J. Wilcox. 2013. "Length of Human Pregnancy and Contributors to Its Natural Variation." *Human Reproduction* 28, no. 10: 2848–2855.

Kurek, M., E. Żądzińska, A. Sitek, B. Borowska-Strugińska, I. Rosset, and W. Lorkiewicz. 2016. "Neonatal Line Width in Deciduous Incisors From Neolithic, Medieval and Modern Skeletal Samples From North-Central Poland." *Annals of Anatomy - Anatomischer Anzeiger* 203: 12–18.

Lewis, M. E. 2006. *Bioarchaeology of Children: Perspectives From Biological and Forensic Anthropology*. Cambridge University Press.

Liversidge, H. M., M. C. Dean, and T. I. Molleson. 1993. "Increasing Human Tooth Length Between Birth and 5.4 Years." *American Journal of Physical Anthropology* 90, no. 3: 307–313.

López-Rey, J. M., Ó. Cambra-Moo, A. González Martín, et al. 2024. "Covariation Between the Shape and Mineralized Tissues of the Rib Cross Section in *Homo Sapiens*, pan Troglodytes and Sts 14." *American Journal of Biological Anthropology* 183, no. 1: 157–164.

López-Rey, J. M., Ó. Cambra-Moo, A. González Martín, et al. 2022. "Mineral Content Analysis in the Rib Cross-Sections of Homo Sapiens and pan Troglodytes and Its Implications for the Study of Sts 14 Costal Remains." *American Journal of Biological Anthropology* 177, no. 4: 784–791.

Malgosa, A., S. Carrascal, G. Piga, and A. Isidro. 2016. "Hip Dislocation and Dystocia in Early Medieval Times: Possible Evidence of Labor Maneuver." *Obstetrics & Gynecology* 128, no. 6: 1384–1387.

Martirosyan, A., C. Sandoval-Ávila, J. Irurita, et al. 2024. "Reconstructing Infant Mortality in Iberian Iron Age Populations From Tooth Histology." *Journal of Archaeological Science* 171: 106088.

Maresh, M. M. 1970. "Measurements From Roentgenograms." In *Human Growth and Development*, edited by R. W. McCammon, 157–200. C. C. Thomas.

McFarlin, S. C., C. J. Terranova, A. L. Zihlman, and T. G. Bromage. 2016. "Primary Bone Microanatomy Records Developmental Aspects of Life History in Catarrhine Primates." *Journal of Human Evolution* 92: 60–79.

Millard, A. R. 2001. "The Deterioration of Bone." In *Handbook of Archaeological Sciences*, edited by D. R. Brothwell and A. M. Pollard, 637–647. John Wiley and Sons Inc.

Molina Moreno, M. 2021. "Muerte y mortalidad perinatal en las poblaciones del pasado. Cambio morfológico e histológico en el desarrollo temprano del esqueleto humano: cuando la estimación de la edad es igual a cero. (Unpublished doctoral dissertation). Universidad Autónoma de Madrid, Madrid."

Monnier, A. 1985. "Les méthodes d'analyse de la mortalité infantile." In *Manuel d'Analyse de la Mortalité*, edited by R. Pressat, 47–59. Institut National d'Études Démographiques, INED.

Moorrees, C. F. A., E. A. Fanning, and E. E. Hunt. 1963. "Age Variation of Formation Stages for Ten Permanent Teeth." *Journal of Dental Research* 42, no. 6: 1490–1502.

Rascón Pérez, J., O. Cambra-Moo, and A. González Martín. 2007. "A Multidisciplinary Approach Reveals an Extraordinary Double Inhumation in the Osteoarchaeological Record." *Journal of Taphonomy* 5, no. 2: 91–101.

Ryan, B. A., and C. S. Kovacs. 2020. "Calciotropic and Phosphotropic Hormones in Fetal and Neonatal Bone Development." *Seminars in Fetal and Neonatal Medicine* 25, no. 1: 101062.

Ryan, S., P. J. Congdon, J. James, J. Truscott, and A. Horsman. 1988. "Mineral Accretion in the Human Fetus." *Archives of Disease in Childhood* 63, no. 7: 799–808.

Scheuer, J. L., J. H. Musgrave, and S. P. Evans. 1980. "The Estimation of Late Fetal and Perinatal Age From Limb Bone Length by Linear and Logarithmic Regression." *Annals of Human Biology* 7, no. 3: 257–265.

Scheuer, L., S. Black, and C. Cunningham. 2000. *Developmental juvenile osteology*, 274–289. 468–469. Academic Press.

Schug, G. R., and H. M. Goldman. 2014. "Birth Is but Our Death Begun: A Bioarchaeological Assessment of Skeletal Emaciation in Immature Human Skeletons in the Context of Environmental, Social, and Subsistence Transition." *American Journal of Physical Anthropology* 155, no. 2: 243–259. https://doi.org/10.1002/ajpa.22536.

Shaw, A. J., M. Z. Mughal, T. Mohammed, M. J. Maresh, and C. P. Sibley. 1990. "Evidence for Active Maternofetal Transfer of Magnesium Across the in Situ Perfused Rat Placenta." *Pediatric Research* 27, no. 6: 622–625.

Stout, S. D., and C. Crowder. 2012. "Bone Remodeling, Histomorphology, and Histomorphometry." In *Bone Histology: An Anthropological Perspective*, edited by C. Crowder and S. Stout, 1–22. CRC Press.

Streeter, M. 2010. "A Four-Stage Method of Age at Death Estimation for Use in the Subadult Rib Cortex." *Journal of Forensic Sciences* 55, no. 4: 1019–1024.

Trotter, M., and B. B. Hixon. 1974. "Sequential Changes in Weight, Density, and Percentage Ash Weight of Human Skeletons From an Early Fetal Period Through Old Age." *Anatomical Record* 179, no. 1: 1–8.

Ubelaker, D. H. 1978. *Human Skeletal Remains, Excavation, Analysis, Interpretation*. Estados Unidos: Taraxacum.

Valencia, V., R. Alba, J. Esquivias, M. Botella, A. Trujillo, and A. Iván. 2020. "Age Determination in Subadults Using Histological Analysis of Bones." *Revista de la Universidad Industrial de Santander. Salud* 52, no. 4: 366–370.

Zanolli, C., L. Bondioli, F. Manni, P. Rossi, and R. Macchiarelii. 2011. "Gestation Length, Mode of Delivery and Neonatal Line-Thickness Variation." *Human Biology* 83, no. 6: 695–713.

Supporting Information

Additional supporting information can be found online in the Supporting Information section.